

The noise of many needles: Jerky domain wall propagation in PbZrO_3 and LaAlO_3

S. Puchberger, V. Soprunyuk, W. Schranz, A. Tröster, K. Roleder, A. Majchrowski, M. A. Carpenter, and E.K.H. Salje

Citation: *APL Materials* **5**, 046102 (2017); doi: 10.1063/1.4979616

View online: <https://doi.org/10.1063/1.4979616>

View Table of Contents: <http://aip.scitation.org/toc/apm/5/4>

Published by the *American Institute of Physics*

Articles you may be interested in

[The noise of the needle: Avalanches of a single progressing needle domain in \$\text{LaAlO}_3\$](#)

Applied Physics Letters **97**, 021907 (2010); 10.1063/1.3460170

[Research Update: Nanoscale electrochemical transistors in correlated oxides](#)

APL Materials **5**, 042303 (2017); 10.1063/1.4974484

[Research Update: Fast and tunable nanoionics in vertically aligned nanostructured films](#)

APL Materials **5**, 042304 (2017); 10.1063/1.4978550

[Evidence for oxygen vacancy manipulation in \$\text{La}_{1/3}\text{Sr}_{2/3}\text{FeO}_3\$ thin films via voltage controlled solid-state ionic gating](#)

APL Materials **5**, 042504 (2017); 10.1063/1.4982249

[Comprehensive biocompatibility of nontoxic and high-output flexible energy harvester using lead-free piezoceramic thin film](#)

APL Materials **5**, 074102 (2017); 10.1063/1.4976803

[Research Update: Ionotronics for long-term data storage devices](#)

APL Materials **5**, 042302 (2017); 10.1063/1.4974480

AIP | Conference Proceedings

**Get 30% off all
print proceedings!**

Enter Promotion Code **PDF30** at checkout



The noise of many needles: Jerky domain wall propagation in PbZrO_3 and LaAlO_3

S. Puchberger,^{1,a} V. Soprunyuk,¹ W. Schranz,¹ A. Tröster,² K. Roleder,³
 A. Majchrowski,⁴ M. A. Carpenter,⁵ and E.K.H. Salje⁵

¹Faculty of Physics, University of Vienna, Boltzmannngasse 5, 1090 Wien, Austria

²Vienna University of Technology, Institute of Material Chemistry, Getreidemarkt 9, 1090 Wien, Austria

³Institute of Physics, University of Silesia, ul. Uniwersytecka 4, 40-007 Katowice, Poland

⁴Institute of Applied Physics, Military University of Technology, ul. Kaliskiego 2, 00-908 Warsaw, Poland

⁵Department of Earth Sciences, University of Cambridge, Downing Street, CB2 3EQ Cambridge, United Kingdom

(Received 1 February 2017; accepted 21 March 2017; published online 5 April 2017)

Measurements of the sample length of PbZrO_3 and LaAlO_3 under slowly increasing force (3–30 mN/min) yield a superposition of a continuous decrease interrupted by discontinuous drops. This strain intermittency is induced by the jerky movement of ferroelastic domain walls through avalanches near the depinning threshold. At temperatures close to the domain freezing regime, the distributions of the calculated squared drop velocity maxima $N(v_m^2)$ follow a power law behaviour with exponents $\varepsilon = 1.6 \pm 0.2$. This is in good agreement with the energy exponent $\varepsilon = 1.8 \pm 0.2$ recently found for the movement of a single needle tip in LaAlO_3 [R. J. Harrison and E. K. H. Salje, *Appl. Phys. Lett.* **97**, 021907 (2010)]. With increasing temperature, $N(v_m^2)$ changes from a power law at low temperatures to an exponential law at elevated temperatures, indicating that thermal fluctuations increasingly enable domain wall segments to unpin even when the driving force is smaller than the corresponding barrier. © 2017 Author(s). All article content, except where otherwise noted, is licensed under a Creative Commons Attribution (CC BY) license (<http://creativecommons.org/licenses/by/4.0/>). [<http://dx.doi.org/10.1063/1.4979616>]

Domain wall (DW) motion in ferroelastic materials subjected to external stress leads to a significant anelastic behavior and superelastic softening.^{1,2} Superelastic softening was measured in many materials, e.g., in SrTiO_3 ,³ LaAlO_3 ,^{4,5} PbZrO_3 ,⁶ $\text{Ca}_{1-x}\text{Sr}_x\text{TiO}_3$,⁷ and KMnF_3 .^{8,9} Most of these materials show rehardening at temperatures $T_f < T_c$, due to freezing of the DW motion at decreasing temperatures. The domain freezing process in ferroelastic materials is a topic of current research.¹⁰ Pinning of DW's to defects like oxygen vacancies and/or dislocations seems to play an important role in this context.^{7,11,12} For ferroelectric materials, domain freezing was already reported much earlier¹³ and was explained by pinning of randomly distributed defects to DW's, which become increasingly collective at low temperatures, leading to a Vogel-Fulcher (VF) type divergence of DW relaxation times.

Large-scale molecular dynamics simulations^{14,15} of a simple two dimensional spring model with a sheared (ferroelastic) ground state show that domain wall movements under applied shear deformation indeed follow the Vogel-Fulcher behavior at a certain temperature-regime. They found that pinning/depinning processes also appear as a consequence of domain jamming even if no external defects are present. Based on the results of these simulations, Salje *et al.*¹⁴ predicted the existence of two distinct regimes of DW movement: a low temperature athermal and a high temperature thermally activated regime. At higher temperatures, thermal activation leads to a Vogel-Fulcher (VF) distribution of avalanches. The slowing down of DW dynamics with decreasing temperature is reminiscent

^aElectronic mail: sabine.puchberger@univie.ac.at

of the glassy behavior and has led to the concept of “domain glass.”¹⁶ Below the VF temperature, the DW's show jerky, athermal movements. Such an intermittent response of a system to slowly changing external conditions was found in many different contexts, e.g., for the motion of ferromagnetic DW's,^{17–19} plastic deformation in metals,^{20–23} phase front or twin propagation at martensitic transitions,^{24–29} cracks in paper fracture,^{30–32} and other crack propagation experiments,³³ as well as at slow compression of nanoporous silica^{34–36} and wood.³⁷

In contrast to these systems, very few experimental data on the intermittent behaviour of ferroelastic domain walls exist. Most experiments on ferroelastic walls have focused on its ballistic character, showing a smooth wall propagation. In a recent experiment, Harrison *et al.*⁴¹ demonstrated that jerky avalanches exist also at ferroelastic DW propagation. They measured the movement of a single needle domain in LaAlO₃ under weak external stress at the critical depinning threshold of domain walls and found discrete jumps of the needle tip of varying amplitude due to the pinning/depinning of walls to defects. They described the movement of a needle domain as a superposition of a smooth front propagation and a stop-and-go propagation of the needle tip. Tracking the movement of the needle tip $x(t)$ yields the dissipated energy via the kinetic energy $E \sim v^2 = (dx/dt)^2$. They found that the distribution of energies follows a power law $P(v^2) \propto (v^2)^{-\varepsilon}$ behavior with an energy exponent of $\varepsilon = 1.8 \pm 0.2$.

The jerky propagation of elastic walls in an external stress field shares some similarities with the behavior of magnetic walls subject to an external magnetic field. During domain switching, avalanches occur which represent the intrinsic noise of this process. In magnetic systems, this characteristic noise is termed Barkhausen noise.^{17,18} The more general term for this phenomenon is crackling noise.^{42,43}

Harrison *et al.*⁴¹ obtained similar exponents for the needle tip motion in LaAlO₃ as found previously in measurements of shape memory alloys ($\varepsilon \approx 2$)^{24,44} and concluded that there is no systematic difference between the power law exponent in a single domain experiment and that of a multidomain system.

Based on this previous study, we decided to investigate the movement of many DW's in LaAlO₃ and PbZrO₃. The most sensitive technique to study microstructural evolutions which produce crackling noise is acoustic emission (AE). Various systems have been investigated by AE including paper fraction,³⁰ porous materials,^{35,36} and martensitic transitions.²⁵ Despite numerous advantages, AE also has its drawbacks, especially for micron-scale samples and ferroic transformations.¹⁶ In addition, ferroelastic twinning is hard to quantify.⁴⁵

The experimental technique employed in the present study involves the measurement of strain drops under slowly increasing external stress ($\approx 0.05 - 5$ kPa/s) with a Dynamical Mechanical Analyzer (Pyris Diamond DMA, Perkin Elmer). The energy distribution of jerks is obtained from the statistical characteristics of height drops $\Delta h(t)$. From the evolution of the sample height $h(t)$, we calculate the squared temporal derivatives $v(t)^2 = (dh/dt)^2$ and determine the distribution of squared maximal drop velocities $N(v_m^2)$. Recently, this method was successfully applied to determine the power law exponent of the energy distribution of collapsing pores in the work of Vycor and Gelsil.³⁴ Using DMA one can apply a force up to 10 N with a resolution of 0.002 N, and the resolution in sample height is about 3 nm. The main advantage of this method is the possibility to measure even micron-scale samples and perform measurements in a broad temperature range ($T = -120^\circ\text{C}$ to $+600^\circ\text{C}$). However, the main disadvantage is the limited time resolution (1s), which is due to the restricted sampling rate of the apparatus. For this reason, we cannot study, e.g., distributions of avalanche durations with this method presently. Here we have chosen to study variables like maximum velocity or squared maximum velocities, which turned out to be not so sensitive³⁴ to the sampling rate.

For our present study, single crystals of lead zirconate and lanthanum aluminate were used. Both perovskite crystals exhibit a phase transition to an improper ferroelastic phase. In LaAlO₃ the structure changes from cubic $\text{Pm}\bar{3}\text{m}$ to rhombohedral $\text{R}\bar{3}\text{c}$ at $T_c = 823$ K⁵. PbZrO₃ undergoes a phase transition⁶ from a paraelectric $\text{Pm}\bar{3}\text{m}$ to an antiferroelectric orthorhombic Pbam phase at $T_c \approx 503$ K. Lead zirconate samples were cut to an approximate size of $1 \times 0.8 \times 0.8$ mm³, mounted between steel rods with parallel faces and slowly compressed at constant force rates. For LaAlO₃ the samples were larger and, therefore, it was possible to cut longer pieces for three-point-bending geometry as well as samples for parallel-plate geometry. The long sample with dimensions of about $5 \times 1.8 \times 0.57$ mm³ was placed on two supports with a distance of 3.6 mm and the loading

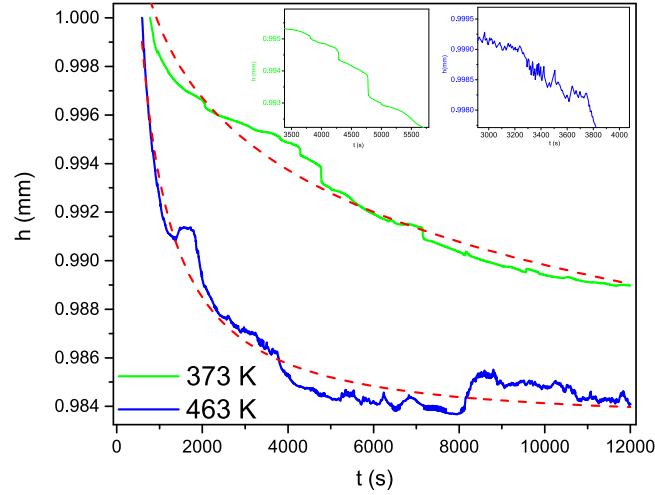


FIG. 1. Height evolution during a compression experiment of PbZrO_3 at 373 K (green) and 473 K (blue). The applied force is increased at a rate of 15 mN/min from 10 to 3000 mN. The dashed red lines correspond to (stretched)-exponential fits. Magnifications of $h(t)$ are shown in insets.

pin applied constant force rates (see the inset of Fig. 2). The parallel plate sample had a size of $2.88 \times 1.78 \times 0.53 \text{ mm}^3$.

First, we performed pre-measurements on these samples to check if the domain walls are movable upon application of a force in the desired direction. The same geometries and sample orientations were then used for subsequent investigations of the crackling behavior (parallel plate for PbZrO_3 and three-point-bending/parallel-plate for LaAlO_3). From previous studies,^{4,6} it is known that using a measurement frequency of 1 Hz, in both cases the domain walls are frozen ($\omega\langle\tau\rangle > 1$) at sufficiently low temperatures, and their mobility starts above 293 K in PbZrO_3 and 373 K in LaAlO_3 . Figures 1 and 2 (green lines) show the discontinuous evolution of the sample heights of PbZrO_3 and LaAlO_3 at very low stress rates of 15 mN/min and 3 mN/min, respectively. Most probably, the height drops are manifestations of pinning/depinning events of domain walls to defects, which presumably are formed by oxygen vacancies.^{4,5} Measurements with stress rates higher than about 35 mN/min resulted in only a few jerks and as a result the squared drop velocities showed no well-defined power-law distribution.

The squared drop velocity (energy) peaks, Figs. 2 and 6, vary over several orders of magnitude and consist of about 13 200 (for LaAlO_3) and 3800 (for PbZrO_3), respectively, single discontinuous strain bursts. 4000 out of 13 200 ($\approx 30\%$) and 400 out of 3800 ($\approx 10\%$) peaks correspond to positive velocity

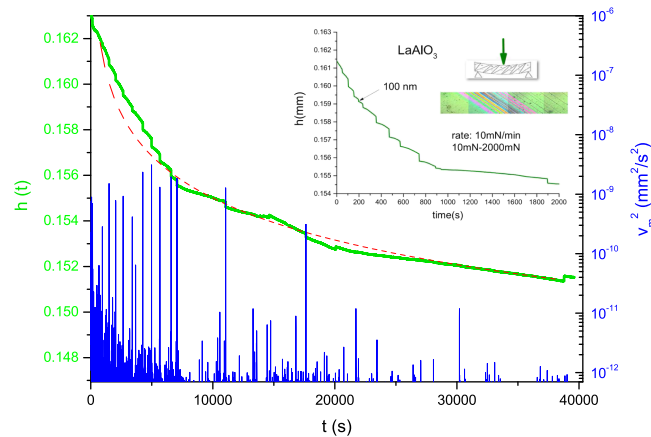


FIG. 2. Compression experiment of LaAlO_3 at 295 K. The green line displays the measured sample height h . The applied force is increased at a rate of 3 mN/min from 10 to 2000 mN. Blue lines show the squared drop velocity maxima $v_m^2 = (dh/dt)_{\text{max}}^2$. The dashed red line corresponds to a (stretched)-exponential fit. The inset shows a sketch of the geometrical situation in the case of three-point-bending setup and magnification of $h(t)$.

jumps, i.e., backward movements of the domain walls. Middleton's theorem^{38,39} states that for purely elastic interactions the interface can only move forward in response to the driving force. Backward jumps in disordered media can occur for *viscoelastic* interfaces.⁴⁰ To account for the possibility of backward movements, we analyzed the data by including backjumps and without backjumps, yielding the same statistical results (Figs. 3 and 4), in good agreement with Ref. 40.

For calculation of the power law exponents, the peak data were logarithmically binned (bin size = 0.1) and plotted in a histogram. Figs. 3 and 4 show log-log plots of the distributions of squared drop velocity maxima, which are fitted according to $N(v_m^2) \propto (v_m^2)^{-\varepsilon}$ with $\varepsilon = 1.6 \pm 0.2$. The same exponent value was obtained for parallel-plate measurements of LaAlO_3 . Furthermore, the exponent value for LaAlO_3 is not far from the results of Harrison and Salje,⁴¹ who obtained an exponent of $\varepsilon = 1.8 \pm 0.2$ for the jerky propagation of one needle. At the present stage, we cannot decide whether the small difference in exponents results from DW interactions or if it is just due to some limitations in experimental resolution.

Further measurements on PbZrO_3 (Fig. 5) at various temperatures ranging from 295 K to 373 K all revealed a jerky evolution of the sample height with power laws in the corresponding squared drop velocity distributions with similar exponent values. At higher temperatures, yet still below the phase

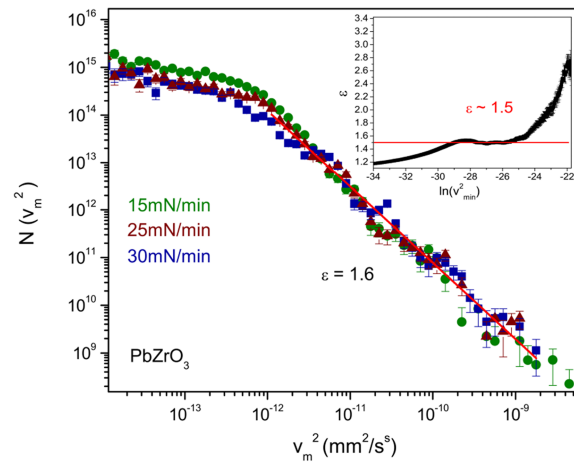


FIG. 3. Log-log plot of the distribution $N(v_m^2)$ of maximum drop velocities squared of PbZrO_3 at different stress rates at 373 K. The red line corresponds to a power law with exponent $\varepsilon = 1.6 \pm 0.1$. The inset shows the corresponding maximum likelihood plot.

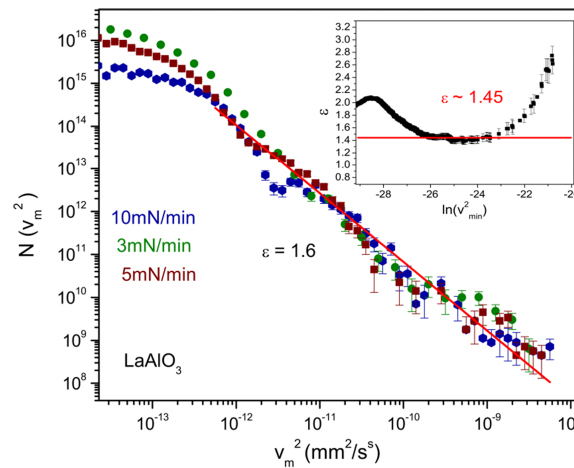


FIG. 4. Log-log plot of the distribution $N(v_m^2)$ of squared maximum drop velocities of LaAlO_3 at room temperature, at different stress rates. The red line corresponds to a power law with exponent $\varepsilon = 1.6 \pm 0.2$. Three-point-bending geometry was used for these measurements. The inset shows the corresponding maximum likelihood plot.

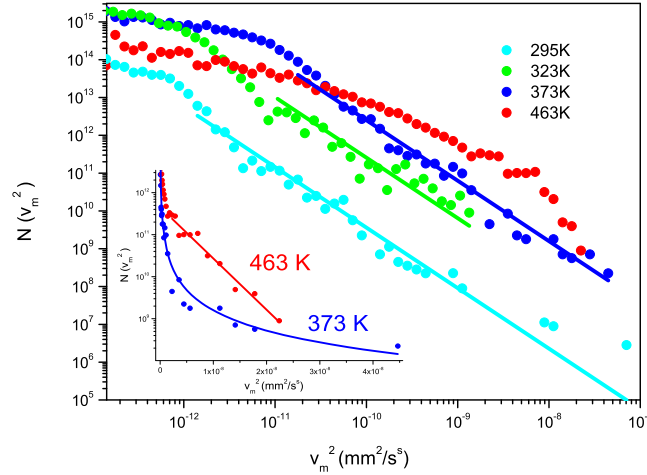


FIG. 5. Log-log plot of the distribution $N(v_m^2)$ of maximum drop velocities squared of PbZrO_3 at different temperatures at a stress rate of 15 mN/min. Curves are shifted for clarity. The inset shows a log-linear plot of the curves at 373 K and 463 K.

transition ($T_c \approx 303$ K), e.g., at 463 K the behavior differs considerably, resulting in an exponential distribution of $N(v_m^2)$.

This observed crossover—which is in agreement with recent computer simulations of a ferroelastic switching process at different temperatures (compare, e.g., with Fig. 2 of Ref. 43)—is most probably due to thermal fluctuations which at a high temperature ease the motion of domain wall segments of various length l_i with a rate of $\tau(l_i)^{-1} = \tau_0^{-1} e^{-E(l_i)/T}$. On average, thermal fluctuations push the interface in the direction of the driving force and the average interface velocity $\langle v \rangle > 0$ even when the applied force F is smaller than the critical depinning force $F < F_c$. Indeed Harrison and Redfern⁴ have shown that the maximum applied force required to unpin DW's in LaAlO_3 decreases drastically with increasing temperature from 800 mN at 370 K to 200 mN at 670 K.

To learn more about the dynamics of the DW segments, we have also analyzed the waiting times t_w between successive events (Figs. 6(a) and 6(b)). One clearly observes an increase in the number of energy jerks from 373 K to 473 K, a behaviour which was also found in computer simulations.¹⁴ It is also reflected in the corresponding power law exponents for the distribution of waiting times $N(t_w) \propto t_w^{-\beta(T)}$, which change from $\beta \approx 2$ at 373 K to $\beta \approx 2.9$ at 473 K implying that long waiting times are increasingly suppressed with increasing temperature. This change of β with T may be understood following the seminal work of V.M. Vinokur⁴⁹ who showed (for an elastic manifold driven through a random medium) that the distribution of waiting times $t_w(l_i) = \tau_0 e^{E(l_i)/T}$ for hops between metastable states scales as a power-law $P(t_w) \propto T t_w^{-\beta(T)}$ with $\beta(T) = 1 + \text{const.} T/U_c$.

In summary, the present work corroborates the physical picture that domain wall motion in ferroelastic materials involves various processes depending on temperature, time, and spatial scale. As can be seen in Figs. 1 and 2, the evolution of the sample height with slowly increasing stress follows a stretched-exponential relaxation envelope interrupted by discrete jumps of varying amplitude, in good agreement with the findings of Refs. 41 and 46. The discrete events are usually associated with pinning by extrinsic defects or intrinsically due to mutual jamming of domain walls.¹⁴ The fact that the corresponding energies are power law distributed indicates a large underlying variety of sizes associated with the jerks. For LaAlO_3 the pinning-depinning process was shown⁴⁶ to be mainly effective at the front line of the needle tips (see, e.g., Fig. 2 in Ref. 46), which is pinned most likely at statistically distributed oxygen vacancies. These rather smooth front lines can easily break into smaller segments of various lengths because they are not subject to elastic compatibility unlike the planar parts of the ferroelastic domain walls, whose Larkin length is very large. The behaviour of the front line is reminiscent of the movement of an elastic string in a random potential.^{47–49} Le Blanc *et al.*^{50,51} calculated the distribution of maximum velocities $P(v_m) \propto v_m^{-\mu}$ and maximum energies ($E_m \equiv v_m^2$), i.e., $P(v_m^2) \propto (v_m^2)^{-\varepsilon}$ in avalanches of a slowly driven elastic interface near the depinning transition.

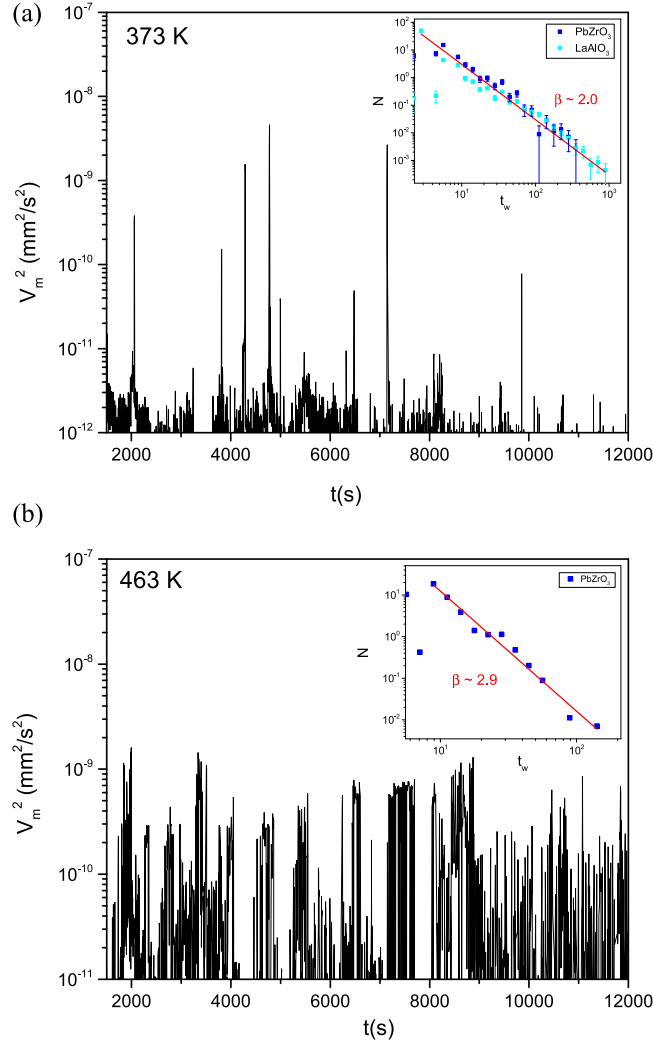


FIG. 6. Squared drop velocity peaks $v_m^2 = (dh/dt)_{\max}^2$ of PbZrO_3 at 373 K (a) and at 473 K (b). Insets show the corresponding waiting time distributions $N(t_w)$ yielding exponent values of $\beta \approx 2$ (a) and $\beta \approx 2.9$ (b). Inset (a) includes also, for comparison, the waiting time distribution of LaAlO_3 at room temperature which at this temperature shows a similar power law behavior as PbZrO_3 at 373 K.

Using the mean-field approximation, they obtained $\mu = 2$ and $\varepsilon = 1.5$. Our values $\varepsilon = 1.6 \pm 0.1$ for PbZrO_3 and $\varepsilon = 1.6 \pm 0.2$ for LaAlO_3 are quite compatible with these mean-field values. On the other hand, the value of $\varepsilon = 1.8 \pm 0.2$ found recently from the movement of one needle^{41,52} and other values $\varepsilon \approx 2$ from acoustic emission measurements of compressed Ti-Ni shape memory alloys⁴⁴ or Ni-Mn-Ga^{27,53} ($\varepsilon = 1.8 \pm 0.2$) indicate some possible deviations from mean-field values. Further studies have to be done to test whether these slight discrepancies are due to interactions between domain walls, nucleation of secondary domains or result from differences in the detection method, i.e., AE vs. strain intermittency measurements,⁵⁴ or due to some limitations of the detection methods.³³

Nevertheless, based on these present first results we conclude that ferroelastic needle shaped domains can act as a model system for the study of elastic strings in random environments.

The present work was supported by the Austrian Science Fund (FWF) Grant Nos. P28672-N36 and P27738-N28, the National Science Centre, Poland, within the project 2016/21/B/ST3/02242, EPSRC Grant No. EP/K009702/1, and Leverhulme trust Grant No. EM-2016-004.

¹ W. Schranz, *Phys. Rev. B* **83**, 094120 (2011).

² W. Schranz, H. Kabelka, A. Sarrao, and M. Burock, *Appl. Phys. Lett.* **101**, 141913 (2012).

³ A. V. Kityk, W. Schranz, P. Sondergeld, D. Havlik, E. K. H. Salje, and J. F. Scott, *Phys. Rev. B* **61**, 946 (2000).

- ⁴ R. J. Harrison and S. A. T. Redfern, *Phys. Earth Planet. Inter.* **134**, 253 (2002).
- ⁵ R. J. Harrison, S. A. T. Redfern, and E. K. H. Salje, *Phys. Rev. B* **69**, 144101 (2004).
- ⁶ S. Puchberger, V. Soprunyuk, A. Majchrowski, K. Roleder, and W. Schranz, *Phys. Rev. B* **94**, 214101 (2016).
- ⁷ R. J. Harrison, S. A. T. Redfern, and J. Street, *Am. Mineral.* **88**, 574 (2003).
- ⁸ W. Schranz, A. Tröster, A. V. Kityk, P. Sondergeld, and E. K. H. Salje, *Europhys. Lett.* **62**, 512 (2003).
- ⁹ W. Schranz, P. Sondergeld, A. V. Kityk, and E. K. H. Salje, *Phys. Rev. B* **80**, 094110 (2009).
- ¹⁰ E. K. H. Salje, X. Wang, X. Ding, and J. Sun, *Phys. Rev. B* **90**, 064103 (2014).
- ¹¹ C. Wang, Q. F. Fang, Y. Shi, and Z. G. Zhu, *Mater. Res. Bull.* **36**, 2657 (2001).
- ¹² K. Roleder, J. Hafiderek, Z. Ujma, and A. Kania, *Ferroelectrics* **70**, 181 (1986).
- ¹³ Y. N. Huang, X. Li, Y. Ding, Y. N. Wang, H. M. Shen, Z. F. Zhang, C. S. Fang, S. H. Zhuo, and P. C. W. Fung, *Phys. Rev. B* **55**, 16159 (1997).
- ¹⁴ E. K. H. Salje, X. Ding, Z. Zhao, T. Lookman, and A. Saxena, *Phys. Rev. B* **83**, 104109 (2011).
- ¹⁵ X. Ding, T. Lookman, Z. Zhao, A. Saxena, J. Sun, and E. K. H. Salje, *Phys. Rev. B* **87**, 094109 (2013).
- ¹⁶ E. K. H. Salje, X. Ding, and O. Aktas, *Phys. Status Solidi B* **251**, 2061 (2014).
- ¹⁷ G. Durin and S. Zapperi, *The Science of Hysteresis*, edited by G. Bertotti and I. Mayergoyz (Elsevier, Amsterdam, 2006), Vol. II, pp. 181–267.
- ¹⁸ F. Colaiori, *Adv. Phys.* **57**, 287 (2008).
- ¹⁹ G. Durin, F. Bohn, M. A. Corrêa, R. L. Sommer, P. Le Doussal, and K. J. Wiese, *Phys. Rev. Lett.* **117**, 087201 (2016).
- ²⁰ D. M. Dimiduk, C. Woodward, R. LeSar, and M. D. Uchic, *Science* **312**, 1188 (2006).
- ²¹ M.-C. Miguel, A. Vespignani, S. Zapperi, J. Weiss, and J.-R. Grasso, *Nature* **410**, 667 (2001).
- ²² A. Vinogradov and I. S. Yasnikov, *Acta Mater.* **70**, 8 (2014).
- ²³ M. Zaiser, J. Schwerdtfeger, A. S. Schneider, C. P. Frick, B. G. Clark, P. A. Gruber, and E. Arzt, *Philos. Mag.* **88**(30–32), 3861 (2008).
- ²⁴ M. C. Gallardo, J. Manchado, F. J. Romero, J. del Cerro, E. K. H. Salje, A. Planes, E. Vives, R. Romero, and M. Stipcich, *Phys. Rev. B* **81**, 174102 (2010).
- ²⁵ J. Baró, J.-M. Martin-Olalla, F. J. Romero, M. C. Gallardo, E. K. H. Salje, E. Vives, and A. Planes, *J. Phys.: Condens. Matter* **26**, 125401 (2014).
- ²⁶ E. K. H. Salje, J. Koppensteiner, M. Reinecker, W. Schranz, and A. Planes, *Appl. Phys. Lett.* **95**, 231908 (2009).
- ²⁷ X. Balandraud, N. Barrera, P. Biscari, M. Grédiac, and G. Zanzotto, *Phys. Rev. B* **91**, 174111 (2015).
- ²⁸ E. Faran, H. Seiner, M. Lanola, and D. Shilo, *Appl. Phys. Lett.* **107**, 171601 (2015).
- ²⁹ E. Faran, E. K. H. Salje, and D. Shilo, *Appl. Phys. Lett.* **107**, 071902 (2015).
- ³⁰ L. I. Salminen, A. I. Tolvanen, and M. J. Alava, *Phys. Rev. Lett.* **89**, 185503 (2002).
- ³¹ S. Santucci, P. P. Cortet, S. Deschanel, L. Vanel, and S. Ciliberto, *Europhys. Lett.* **74**(4), 595 (2006).
- ³² M. Stojanova, L. Vanel, and O. Ramos, *Phys. Rev. Lett.* **112**, 115502 (2014).
- ³³ S. Janičević, L. Laurson, K. J. Møløy, S. Santucci, and M. J. Alava, *Phys. Rev. Lett.* **117**, 230601 (2016).
- ³⁴ V. Soprunyuk, W. Schranz, A. Tröster, S. Puchberger, E. Vives, and E. K. H. Salje, “Avalanches in functional materials and Geophysics,” in *Understanding Complex Systems*, edited by E. K. H. Salje, A. Saxena, and A. Planes (Springer, 2016).
- ³⁵ J. Baró, Á. Corral, X. Illa, A. Planes, E. K. H. Salje, W. Schranz, D. E. Soto-Parra, and E. Vives, *Phys. Rev. Lett.* **110**, 088702 (2013).
- ³⁶ G. F. Nataf, P. O. Castillo-Villa, J. Baró, X. Illa, E. Vives, and A. Planes, *Phys. Rev. B* **90**, 022405 (2014).
- ³⁷ T. Mäkinen, A. Miksic, M. Ovaska, and M. J. Alava, *Phys. Rev. Lett.* **115**, 055501 (2016).
- ³⁸ A. A. Middleton, *Phys. Rev. Lett.* **68**, 670 (1992).
- ³⁹ Y. Liu and K. A. Dahmen, *Phys. Rev. E* **76**, 031106 (2007).
- ⁴⁰ F. P. Landes, “Viscoelastic interfaces in disordered media and applications to friction,” Ph.D. thesis, Université Paris-Sud, 2014, page 111.
- ⁴¹ R. J. Harrison and E. K. H. Salje, *Appl. Phys. Lett.* **97**, 021907 (2010).
- ⁴² J. P. Sethna, K. A. Dahmen, and C. R. Myers, *Nature* **410**, 242 (2001).
- ⁴³ X. He, X. Ding, J. Sun, and E. K. H. Salje, *Appl. Phys. Lett.* **108**, 072904 (2016).
- ⁴⁴ D. Soto-Parra, X. Zhang, S. Cao, E. Vives, E. K. H. Salje, and A. Planes, *Phys. Rev. E* **91**, 060401 (2015).
- ⁴⁵ E. Dul’kin, E. K. H. Salje, O. Aktas, R. W. Whatmore, and M. Roth, *Appl. Phys. Lett.* **105**, 212901 (2014).
- ⁴⁶ R. J. Harrison and E. K. H. Salje, *Appl. Phys. Lett.* **99**, 151915 (2011).
- ⁴⁷ P. Chauve, T. Giamarchi, and P. Le Doussal, *Phys. Rev. B* **62**, 6241 (2000).
- ⁴⁸ A. B. Kolton, A. Rosso, T. Giamarchi, and W. Krauth, *Phys. Rev. B* **79**, 184207 (2009).
- ⁴⁹ V. M. Vinokur, *Physica D* **107**, 411 (1997).
- ⁵⁰ M. LeBlanc, L. Angheluta, K. Dahmen, and N. Goldenfeld, *Phys. Rev. E* **87**, 022126 (2013).
- ⁵¹ M. LeBlanc, L. Angheluta, K. Dahmen, and N. Goldenfeld, *Phys. Rev. Lett.* **109**, 105702 (2012).
- ⁵² E. K. H. Salje and K. A. Dahmen, *Annu. Rev. Condens. Matter Phys.* **5**, 233 (2014).
- ⁵³ R. Niemann, J. Kopeček, O. Heczko, J. Romberg, L. Schultz, S. Fähler, E. Vives, L. Mañosa, and A. Planes, *Phys. Rev. B* **89**, 214118 (2014).
- ⁵⁴ V. Navas-Portella, Á. Corral, and E. Vives, *Phys. Rev. E* **94**, 033005 (2016).